

1 **5-Deoxyadenosine Salvage by Promiscuous Enzyme Activity**  
2 **leads to Bioactive Deoxy-Sugar Synthesis in**  
3 ***Synechococcus elongatus***

4  
5 **Running title: Unusual 5-deoxyadenosine salvage in *S. elongatus***

6  
7 Johanna Rapp<sup>a</sup>, Pascal Rath<sup>b</sup>, Joachim Kilian<sup>c</sup>, Klaus Brilisauer<sup>a</sup>, Stephanie Grond<sup>b</sup>, Karl  
8 Forchhammer<sup>a#</sup>

9 <sup>a</sup>Interfaculty Institute of Microbiology and Infection Medicine, Microbiology/Organismic Interactions, Eberhard  
10 Karls Universität Tübingen, Auf der Morgenstelle 28, 72076 Tübingen, Germany.

11 <sup>b</sup>Institute of Organic Chemistry, Eberhard Karls Universität Tübingen, Auf der Morgenstelle 18, 72076 Tübingen,  
12 Germany.

13 <sup>c</sup>Center for Plant Molecular Biology, Eberhard Karls Universität Tübingen, Auf der Morgenstelle 32, 72076  
14 Tübingen, Germany.

15  
16 #corresponding author (karl.forchhammer@uni-tuebingen.de, Tel.: +49 (7071) 29- 72096)

17  
18 **Abbreviations:** SAM: S-Adenosylmethionine; MTA: Methylthioadenosine; 5dAdo:  
19 5-Deoxyadenosine; MSP: Methionine salvage pathway; 5dR: 5-Deoxyribose; 7dSh:  
20 7-Deoxysedoheptulose; 5dR-1P: 5-Deoxyribose 1-phosphate; 5dRu-1P: 5-Deoxyribulose  
21 1-phosphate; MTRI: Methylthioribose 1-phosphate isomerase; MTR: Methylthioribose

22  
23 **Keywords:** 5-Deoxyadenosine salvage, 5-deoxyribose, 7-deoxysedoheptulose, 7dSh  
24 biosynthesis; enzyme promiscuity, S-adenosylmethionine, radical SAM enzymes,  
25 cyanobacteria

## 26 **Abstract**

27 7-Deoxysedoheptulose is an unusual deoxy-sugar, which acts as antimetabolite of the  
28 shikimate pathway thereby exhibiting antimicrobial and herbicidal activity. It is produced by  
29 the unicellular cyanobacterium *Synechococcus elongatus* PCC 7942, which has a small, stream-  
30 lined genome, assumed to be free from gene clusters for secondary metabolite synthesis. In  
31 this study, we identified the pathway for the synthesis of 7-deoxysedoheptulose. It originates  
32 from 5-deoxyadenosine, a toxic byproduct of radical *S*-adenosylmethionine (SAM) enzymes,  
33 present in all domains of life. Thereby we identified a novel 5-deoxyadenosine salvage  
34 pathway, which first leads to the synthesis and excretion of 5-deoxyribose and subsequently  
35 of 7-deoxysedoheptulose. Remarkably, all reaction steps are conducted by promiscuous  
36 enzymes. This is a unique example for the synthesis of a bioactive compound without involving  
37 a specific gene cluster. This challenges the view on bioactive molecule synthesis by extending  
38 the range of possible compounds beyond the options predicted from secondary metabolite  
39 gene clusters.

## 40 Introduction

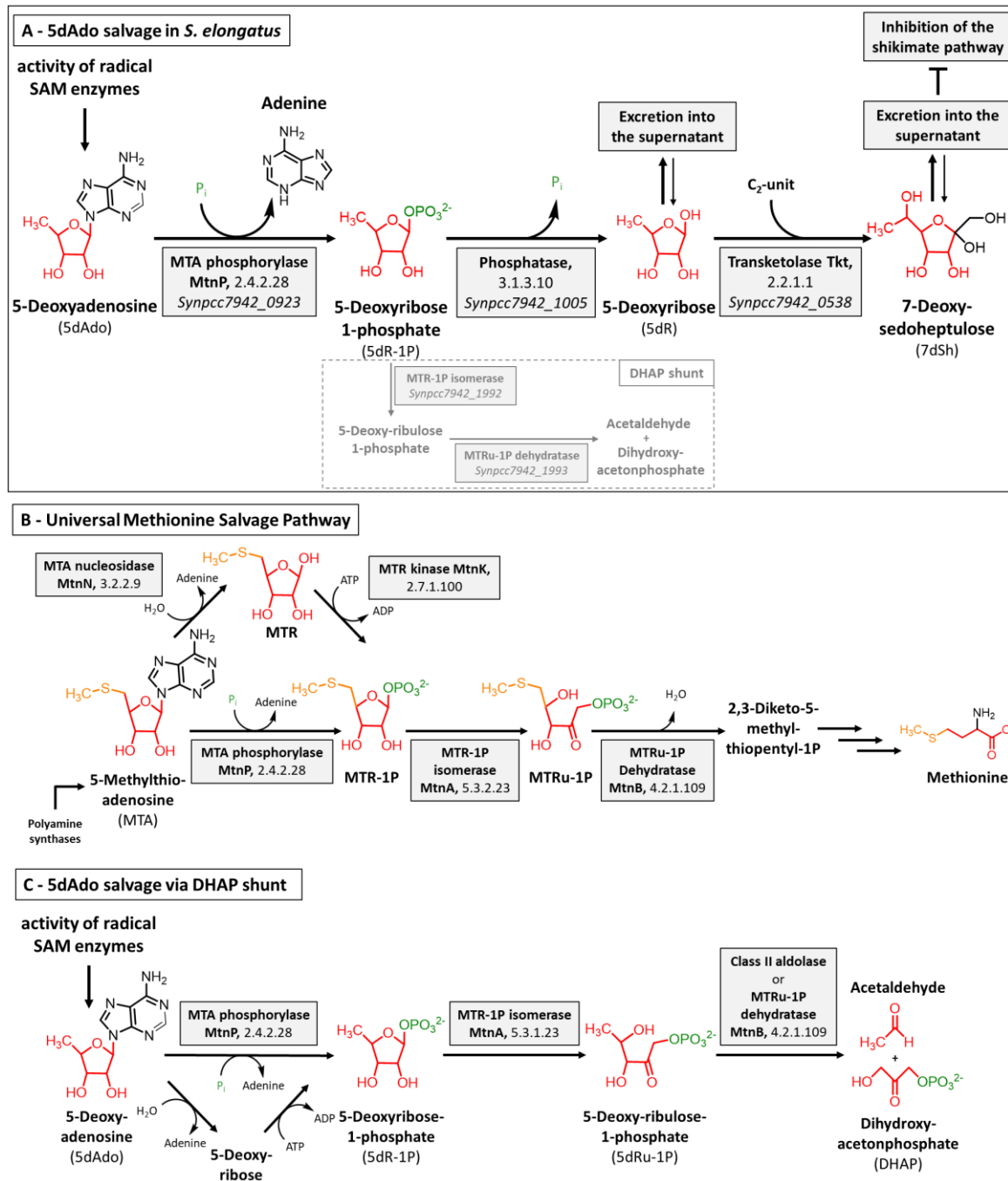
41 S-Adenosyl-L-methionine (SAM or AdoMet), which is formed by ATP and the amino acid  
42 methionine, is an essential cofactor of various enzymatic reactions in all domains of life. SAM  
43 can serve as a methyl group donor for the methylation of DNA, RNA and proteins in reactions  
44 that release S-adenosylhomocysteine (SAH) as byproduct (**Fontecave et al., 2004**). SAM can  
45 also serve as an aminopropyl donor for polyamine synthesis, and as a homoserine lactone  
46 donor for the synthesis of quorum sensing compound N-acetylhomoserine lactone which both  
47 result in the release of 5-methylthioadenosine (MTA). Furthermore, SAM is a source of the  
48 5-deoxyadenosyl radical (5dAdo<sup>\*</sup>), which is formed by the activity of radical SAM enzymes  
49 (**Booker and Grove, 2010; Broderick et al., 2014; Fontecave et al., 2004; Sofia et al., 2001;**  
50 **Wang and Frey, 2007**). 5dAdo<sup>\*</sup> is formed by the reductive cleavage of SAM and can abstract  
51 a hydrogen atom from its substrate to form a substrate radical as well as 5-deoxyadenosine  
52 (5dAdo), which is released as a byproduct (**Marsh et al., 2010; Wang and Frey, 2007**). Radical  
53 SAM enzymes, a superfamily with over 100.000 members, are present in all domains of life  
54 (**Holliday et al., 2018; Sofia et al., 2001**). They are catalysing various complex chemical  
55 reactions, including sulphur insertion, anaerobic oxidations, unusual methylations and ring  
56 formations (**Parveen and Cornell, 2011**). Prominent members of this family are, for example,  
57 involved in biotin, thiamine and lipoate biosynthesis. Other members are involved in DNA  
58 repair or in the biosynthesis of secondary metabolites e.g. antibiotics (**Wang and Frey, 2007**).  
59 MTA, SAH and 5dAdo are product inhibitors of these reactions (**Challand et al., 2009; Choi-**  
60 **Rhee and Cronan, 2005; Farrar et al., 2010; Palmer and Downs, 2013; Parveen and Cornell,**  
61 **2011**). Therefore, and because of the high bioenergetic costs of these compounds, salvage  
62 pathways are necessary. SAH is rescued via the methionine cycle (**North et al., 2020**). MTA  
63 salvage via the methionine salvage pathway (MSP) is also well characterised (**Sekowska and**  
64 **Danchin, 2002; Wray and Abeles, 1995**) (see Figure 1 B). In the classical, aerobic MSP, MTA is  
65 either processed by a two step-reaction by the MTA nucleosidase (MtnN), followed by a  
66 phosphorylation by the MTR kinase (MtnK) or by the MTA phosphorylase (MtnP). The  
67 subsequent reactions consist of a dehydration (MtnB, MTR-1P dehydratase), enolization and  
68 phosphorylation (either by MtnC or by MtnW and MtnX), deoxygenation (MtnD) and a final  
69 transamination step (MtnE) (**Sekowska et al., 2004**).

70 Despite the high abundance of radical SAM enzymes and thereby of 5dAdo, less is known  
71 about 5dAdo salvage. *In vitro* experiments showed that 5dAdo can be processed by a two-step  
72 reaction, in which 5dAdo is cleaved by the promiscuous MTA nucleosidase resulting in the  
73 release of adenine and 5-deoxyribose (5dR) (**Challand et al., 2009; Choi-Rhee and Cronan,**  
74 **2005**). The subsequent phosphorylation of 5dR by MtnK results in the formation of  
75 5-deoxyribose 1-phosphate (5dR-1P). The second option is the direct conversion of 5dAdo into  
76 5dR-1P and adenine via the promiscuous MTA phosphorylase (**Savarese et al., 1981**).  
77 Therefore, Sekowska and coworkers suggested that 5dAdo salvage is paralogous to the MSP  
78 and is driven by the promiscuous activity of the enzymes of the MSP (**Sekowska et al., 2018**).  
79 Recently, a pathway for 5dR salvage was elucidated in *Bacillus thuringiensis* involving the  
80 sequential activity of a kinase (DrdK), an isomerase (DrdI) and a class II aldolase (DrdA), which  
81 are encoded by a specific gene cluster (**Beaudoin et al., 2018**). The authors propose that 5dR  
82 is phosphorylated to 5dR-1P, which is then isomerized into 5-deoxyribulose 1-phosphate  
83 (5dRu-1P) and subsequently cleaved by an aldolase into acetaldehyde and dihydroxyacetone  
84 phosphate (DHAP) for primary metabolism. In organisms that lack the specific gene cluster,  
85 the cleavage of 5dAdo into DHAP and acetaldehyde is proposed to occur via the promiscuous  
86 activity of enzymes of the MSP. In support of this hypothesis, it was shown that  
87 *Arabidopsis thaliana* DEP1, a MTR-1P dehydratase of the MSP, is promiscuous and can also  
88 cleave 5dRu-1P into DHAP and acetaldehyde, suggesting that a specific aldolase is not required  
89 for 5dAdo salvage (**Beaudoin et al., 2018**). In agreement with this, the promiscuous activity of  
90 MSP enzymes in the 5dAdo salvage was recently reported in *Methanocaldococcus jannaschii*  
91 (*M. jannaschii*) (**Miller et al., 2018**). Methylthioribose 1-phosphate isomerase (MTRI) was  
92 shown to use the substrates MTR-1P, 5dR-1P and 5dR. And only recently, it was demonstrated  
93 that 5dAdo is processed to DHAP and acetaldehyde by the first enzymes of the MSP and a  
94 clustered class II aldolase in *Rhodospirillum rubrum* and pathogenic *Escherichia coli* strains, in  
95 a process they called the “DHAP shunt” (**North et al., 2020**) (see Figure 1 C).

96 In our previous work, we isolated the rare deoxy-sugar – namely 7-deoxysedoheptulose  
97 (7-deoxy-D-*altro*-2-heptulose, 7dSh) – from the supernatant of the unicellular cyanobacterium  
98 *Synechococcus elongatus* PCC 7942 (henceforth referred to as *S. elongatus*) (**Brilisauer et al.,**  
99 **2019**). This compound showed bioactivity towards various prototrophic organisms, e.g. other  
100 cyanobacteria, especially *Anabaena variabilis* ATCC 29413 (henceforth referred to as  
101 *A. variabilis*), *Saccharomyces* and *Arabidopsis*. We hypothesized that 7dSh is an inhibitor of

102 the enzyme dehydroquinate synthase (DHQS, EC 4.2.3.4) (**Brilisauer et al., 2019**), the second  
103 enzyme of the shikimate pathway. Because of the streamlined genome of *S. elongatus* and  
104 the lack of specific gene clusters for the synthesis of secondary metabolites (**Copeland et al.,**  
105 **2014; Shih et al., 2013**) the pathway for 7dSh synthesis remained enigmatic. It is worth to  
106 mention that 7dSh was also isolated from the supernatant of *Streptomyces setonensis*  
107 (**Brilisauer et al., 2019; Ito et al., 1971**). Even in this species, a pathway for 7dSh biosynthesis  
108 has remained unresolved. We speculated that 7dSh might be synthesized via primary  
109 metabolic pathways due to enzyme promiscuity. Enzyme promiscuity, the ability of an enzyme  
110 to use various substrates, is especially important for organisms with a small genome.  
111 Previously it was described that the marine cyanobacterium *Prochlorococcus* uses a single  
112 promiscuous enzyme that can transform up to 29 different ribosomally synthesized peptides  
113 into an arsenal of polycyclic bioactive products (**Li et al., 2010**). As from the 7dSh-containing  
114 supernatant of *S. elongatus* we additionally isolated the deoxy-sugar 5-deoxy-D-ribose (5dR),  
115 we hypothesized that 5dR could serve as a putative precursor molecule of 7dSh (**Brilisauer et**  
116 **al., 2019**). *In vitro*, 5dR can serve as a substrate for a transketolase-based reaction, in which a  
117 C<sub>2</sub>-unit (e.g. from hydroxypyruvate) is transferred to the C<sub>5</sub>-unit (3*S*, 4*R* configured) leading  
118 to the formation of 7dSh (**Brilisauer et al., 2019**).

119 In this work we identified the pathway for 7dSh biosynthesis, which involves a new salvage  
120 route for 5dAdo resulting in the release of 5dR and 7dSh in the culture medium. Therefore,  
121 *S. elongatus* can synthesize an allelopathic inhibitor from the products of the primary  
122 metabolism by using promiscuous enzymes.



123

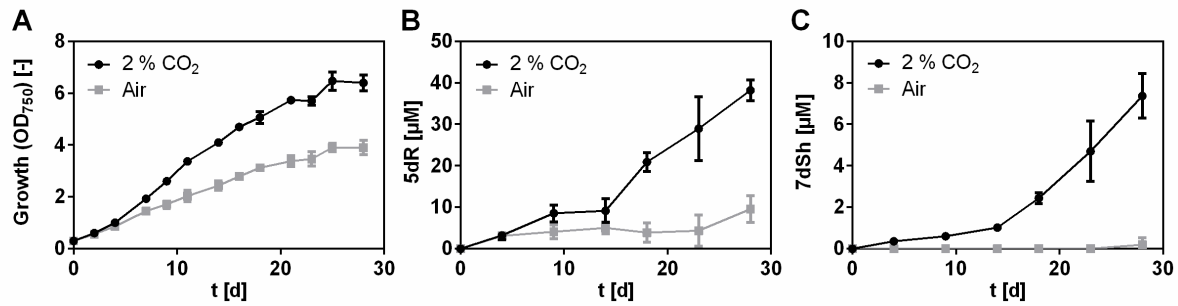
124 **Figure 1: Overview of the 5dAdo and MTA salvage pathways.** (A) - 5dAdo salvage in  
 125 *Synechococcus elongatus* via the excretion of the bioactive deoxy-sugars 5dR and 7dSh (this  
 126 study). 5dR-1P is partially also metabolized via the DHAP shunt (shown by dashed line),  
 127 especially under low carbon conditions. (B) - Universal methionine salvage pathway (MSP)  
 128 (*Sekowska et al., 2004*). MTR: Methylthioribose, MTRu-1P: Methylthioribulose-1P, (C) - 5dAdo  
 129 salvage via the DHAP shunt (*Beaudoin et al., 2018; North et al., 2020*).

## 130 **Results**

### 131 **5dR and 7dSh accumulation in supernatants of *S. elongatus* is strongly promoted by CO<sub>2</sub>** 132 **supplementation**

133 Previously we estimated the content of 7dSh in the supernatant of *S. elongatus* cultures via a  
134 bioassay based on the size of the inhibition zone of *A. variabilis* exposed to the supernatant  
135 of *S. elongatus* (**Brilisauer et al., 2019**). The content of 5dR was neither estimated nor  
136 quantified before. To decipher the biosynthesis of 5dR and 7dSh in *S. elongatus*, we developed  
137 a gas chromatography-mass spectrometry (GC-MS)-based method that enables the detection  
138 and absolute quantification of low  $\mu\text{M}$  concentrations of these metabolites in the supernatant  
139 of cyanobacterial cultures (see Material and Methods). Briefly, 200  $\mu\text{L}$  of culture supernatant  
140 were lyophilized and extracted with chloroform, methanol, and H<sub>2</sub>O. Subsequently, the polar  
141 phase was chemically derivatised with methoxylamine and MSTFA for GC-MS analysis. As  
142 already reported (**Brilisauer et al., 2019**), 7dSh accumulation in the supernatant requires  
143 elevated CO<sub>2</sub> supply to the cultures (Figure 2 C). Under 2 % CO<sub>2</sub> supplementation, 5dR  
144 gradually accumulated with increasing optical density of the cultures, whereas 7dSh  
145 accumulation only started during a later growth phase. After 30 days of growth, the amount  
146 of 7dSh in the supernatant was around one quarter compared to that of 5dR. 5dR  
147 accumulation was strongly promoted by CO<sub>2</sub> supplementation, however, a small amount  
148 already started to accumulate in the cultures under ambient air conditions (Figure 2 B).

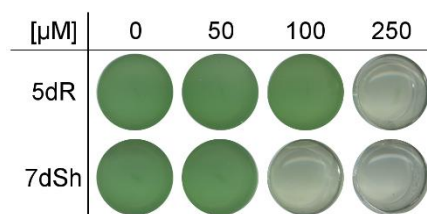
149 Although the optical density of the aerated cultures in the last days of the experiment reached  
150 values that were similar to those of the CO<sub>2</sub>-supplemented cultures, where 7dSh accumulation  
151 started, 7dSh could never be detected in air-grown cultures. This suggests that the formation  
152 of the deoxy-sugars is not only dependent on a certain cell density, but is also related to a  
153 specific metabolic state.



154

155 **Figure 2: 5dR and 7dSh accumulation in the supernatant of *S. elongatus* is strongly promoted**  
156 **by high CO<sub>2</sub> concentrations.** *S. elongatus* cultures aerated either with ambient air (grey  
157 squares) or with air supplemented with 2 % CO<sub>2</sub> (black dots). (A) Over time growth of  
158 *S. elongatus* (indicated by OD<sub>750</sub>). Over time concentration of 5dR (B) or 7dSh (C) in the  
159 supernatant of *S. elongatus* cultures. Note the different values of the y-axis. Data shown  
160 represent mean and standard deviation of three independent biological replicates.

161 To gain further insights into 5dR/7dSh metabolism, we measured the intracellular  
162 concentration of 5dR and 7dSh over the whole cultivation process but were hardly able to  
163 detect any of either deoxy-sugar (Figure S1). Moreover, the small intracellular amount  
164 remained nearly constant while the extracellular concentration increased. The fact that 5dR  
165 and 7dSh only accumulate in the supernatant but is almost undetectable intracellularly  
166 strongly suggests that extracellular 5dR/7dSh accumulation is not due to cell lysis but due to  
167 secretion of the compounds immediately after their formation. Removal of these metabolites  
168 from the cytoplasm is probably essential for *S. elongatus* as both molecules showed growth  
169 inhibition towards the producer strain at elevated concentrations (Figure 3). 7dSh is  
170 bactericidal at concentrations of 100 µM, while 5dR is bacteriostatic at concentrations of  
171 250 µM.



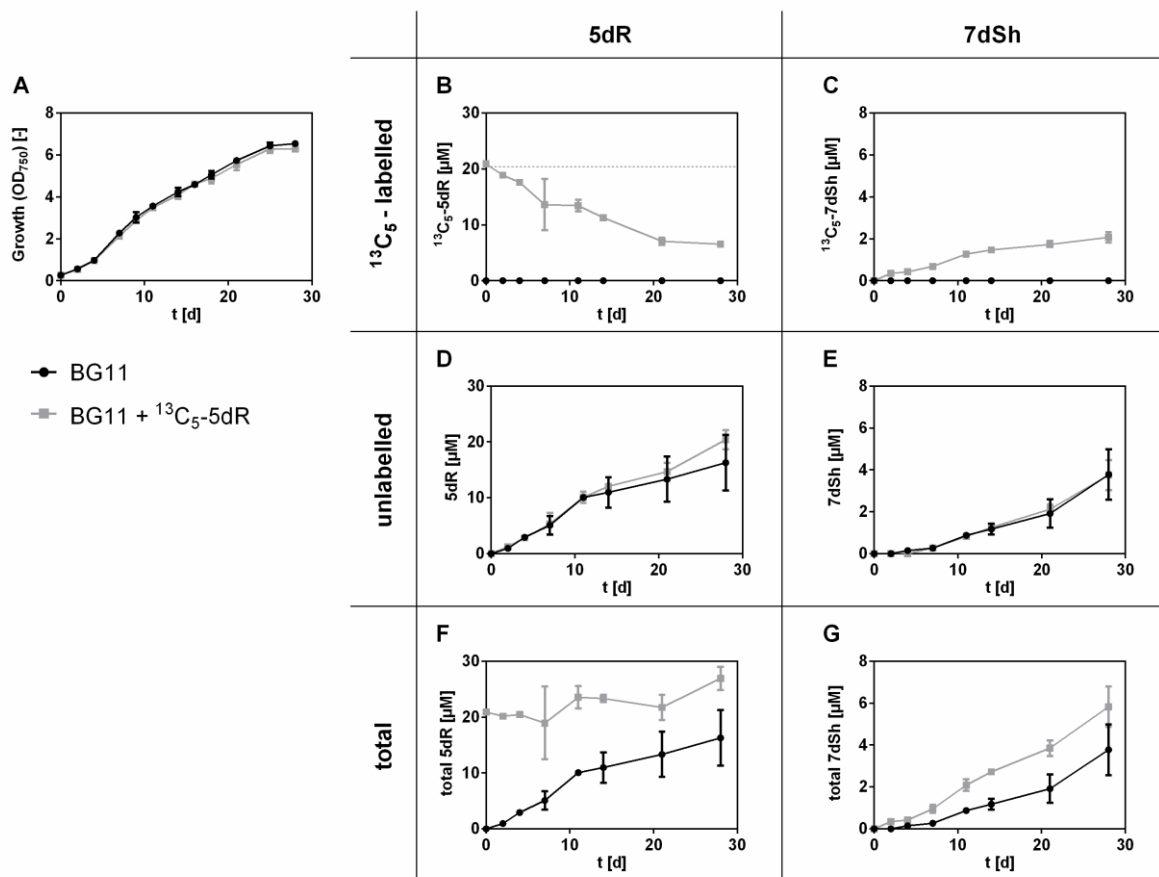
172

173 **Figure 3: 5dR and 7dSh are inhibiting the growth of the producer strain.** Effect of different  
174 concentrations of 5dR and 7dSh on the growth of *S. elongatus*. The cultures were inoculated  
175 at OD<sub>750</sub> = 0.1 in 1 mL BG11 medium in the absence (0) or presence of either 5dR or 7dSh at  
176 the indicated concentrations and grown in a 24-well plate for 3 days. The experiment was  
177 performed in triplicates. The results of one replicate are shown.



178 **5dR is a precursor molecule for 7dSh biosynthesis *in vivo***

179 In our previous work, we reported the *in vitro* synthesis of 7dSh by converting 5dR into 7dSh  
 180 by a transketolase-based reaction with hydroxypyruvate as a C<sub>2</sub>-unit donor (*Brilisauer et al.,*  
 181 **2019**). To determine whether 5dR might also be a precursor molecule for 7dSh *in vivo*, a 5dR-  
 182 feeding experiment was performed (Figure 4). To unambiguously distinguish the naturally  
 183 formed and the supplemented 5dR, uniformly labelled [U-<sup>13</sup>C<sub>5</sub>]-5dR (<sup>13</sup>C<sub>5</sub>-5dR) was  
 184 synthesized and added at a final concentration of 20 μM to *S. elongatus* cultures at the  
 185 beginning of the cultivation. The concentration of labelled (Figure 4 B, C), unlabelled  
 186 (Figure 4 D, E) and the total amount of 5dR and 7dSh (Figure 4 F, G) was determined by GC-MS  
 187 at different time points over a period of 30 days.



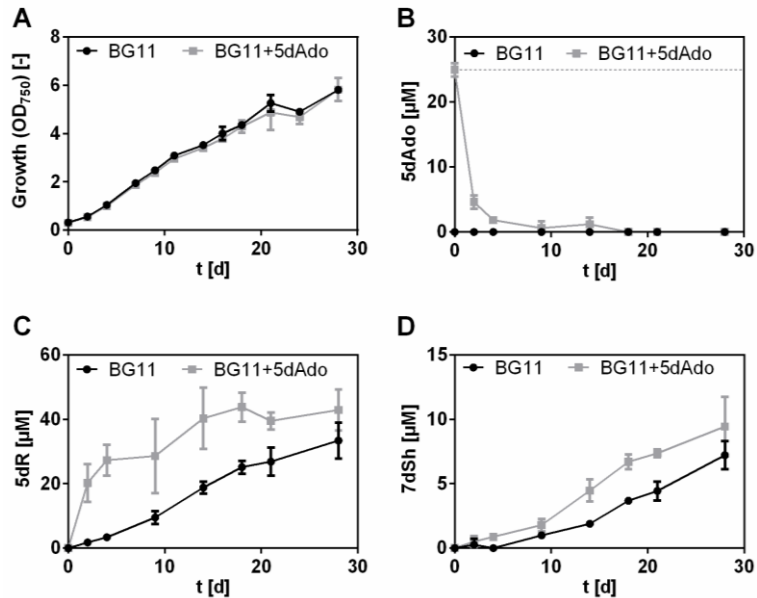
188  
 189 **Figure 4: 5dR is the precursor molecule of 7dSh.** Effects of <sup>13</sup>C<sub>5</sub>-5dR supplementation over the  
 190 time on the growth of *S. elongatus* (A) or on the concentration of <sup>13</sup>C<sub>5</sub>-5dR (B), <sup>13</sup>C<sub>5</sub>-7dSh (C),  
 191 unlabelled 5dR (D), unlabelled 7dSh (E), total 5dR (F) and total 7dSh (G) in the culture  
 192 supernatant. 20 μM <sup>13</sup>C<sub>5</sub>-5dR (indicated by dashed line) was added at the beginning of the  
 193 cultivation (grey squares). Control cultures (black dots) were cultivated in BG11 without  
 194 supplemented <sup>13</sup>C<sub>5</sub>-5dR. All cultures were aerated with air supplemented with 2 % CO<sub>2</sub>. Values  
 195 shown in the graphs represent mean and standard deviation of three biological replicates.

196 Neither the growth of *S. elongatus* nor the excretion of unlabelled, intracellular synthesized  
197 5dR and 7dSh was affected by the addition of exogenous  $^{13}\text{C}_5$ -5dR (Figure 4 A, D, E). We found  
198 that  $^{13}\text{C}_5$ -5dR is taken up by the cultures as its concentration in the supernatant continuously  
199 decreased (Figure 4 B, grey squares). Already within 2 days,  $^{13}\text{C}_5$ -7dSh could be detected in the  
200 supernatant of these cultures (Figure 4 C, grey squares), clearly proving that  $^{13}\text{C}_5$ -7dSh was  
201 formed from the precursor molecule  $^{13}\text{C}_5$ -5dR. However, only a small amount of exogenously  
202 added  $^{13}\text{C}_5$ -5dR was converted into 7dSh. At the end of the experiment, 10 % of the initially  
203 applied  $^{13}\text{C}_5$ -5dR (20  $\mu\text{M}$ ) was converted into  $^{13}\text{C}_5$ -7dSh (around 2  $\mu\text{M}$ ). Around 30 % of  
204  $^{13}\text{C}_5$ -5dR remained in the supernatant (6.5  $\mu\text{M}$ ). The residual amount is assumed to be  
205 metabolised via (an)other pathway(s). Because unlabelled 5dR was excreted at the same time  
206 as  $^{13}\text{C}_5$ -5dR was taken up (Figure 4 B, D), we conclude that 5dR must be imported and exported  
207 in parallel.

208

#### 209 **5dAdo as a precursor molecule of 7dSh**

210 Next, we asked the question where 5dR is derived from and this drew our attention to 5dAdo,  
211 a byproduct of radical SAM enzymes (**Wang and Frey, 2007**). The compound has to be  
212 removed because of its intracellular toxicity (**Choi-Rhee and Cronan, 2005**), and its cleavage  
213 can result in the formation of 5dR (**Beaudoin et al., 2018; Choi-Rhee and Cronan, 2005**) (see  
214 Figure 1 C). To prove the hypothesis that 7dSh is formed as a result of 5dAdo salvage in  
215 *S. elongatus*, 5dAdo feeding experiments were performed and the supernatants were  
216 analysed by GC-MS (Figure 5). Notably, the growth of *S. elongatus* was not affected by  
217 supplementation with 5dAdo, which was taken up very quickly (Figure 5 A, B). After 4 days,  
218 almost all 5dAdo was taken up. A control experiment showed that the rapid decline in the  
219 amount of 5dAdo in the supernatant was not caused by the instability of 5dAdo in the  
220 medium. Feeding of the cells with 5dAdo immediately led to an enhanced accumulation of  
221 5dR in the culture supernatant (Figure 5 C). After 14 days, 7dSh accumulation in 5dAdo-  
222 supplemented cultures was clearly enhanced in comparison to control cultures (Figure 5 D),  
223 supporting our hypothesis that 5dAdo is a precursor molecule of 7dSh. This experiment also  
224 revealed that only about half of the supplemented 5dAdo (initial concentration: 25  $\mu\text{M}$ ) is  
225 converted into 5dR and 7dSh, because at the end of the growth experiment the 5dR content  
226 in the supplemented cultures is increased by around 10  $\mu\text{M}$ , and that of 7dSh by 2  $\mu\text{M}$ . This  
227 suggest that other pathway(s) for 5dAdo salvage must exist.

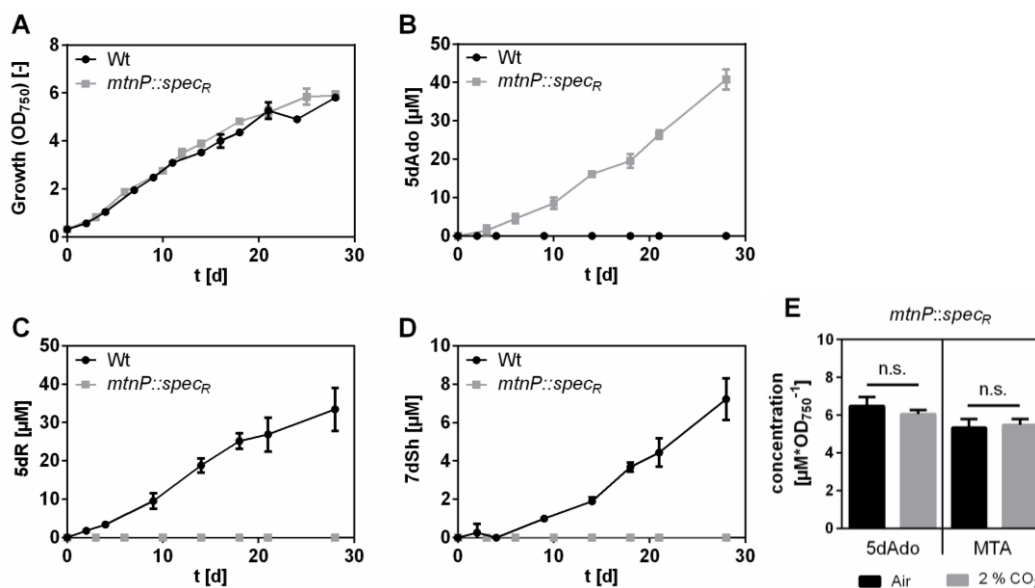


228

229 **Figure 5: 5dAdo feeding experiment.** Effect of 5dAdo-supplementation on the growth of  
230 *S. elongatus* (A) or on the concentration of 5dAdo (B), 5dR (C) and 7dSh (D) in the culture  
231 supernatant. 25  $\mu\text{M}$  5dAdo (indicated by dashed line) was added at the beginning of the  
232 cultivation (grey squares). Control cultures (black dots) were cultivated in BG11 in absence of  
233 exogenous 5dAdo. All cultures were aerated with air supplemented with 2 % CO<sub>2</sub>. Note the  
234 different values of the y-axis. Values shown in the graphs represent mean and standard  
235 deviation of three biological replicates.

236 5dAdo is known to be cleaved either by the MTA nucleosidase (MtnN) or by the MTA  
237 phosphorylase (MtnP) (*Challand et al., 2009; Choi-Rhee and Cronan, 2005; Savarese et al.,*  
238 *1981*). The first reaction leads to the release of adenine and 5dR, the latter is phosphate-  
239 dependent and leads to the release of adenine and 5dR-1P. In *S. elongatus*, no homologous  
240 gene for a MTA nucleosidase was found, but gene *Synpcc7942\_0923* is annotated as a MTA  
241 phosphorylase. Therefore, an insertion mutant of *Synpcc7942\_0923* was generated via the  
242 replacement of the gene by an antibiotic resistance cassette (*S. elongatus mtnP::spec<sub>R</sub>*). Under  
243 conditions favourable for 5dR/7dSh production the mutant grew like the wild type  
244 (Figure 6 A). A GC-MS analysis of the culture supernatant revealed that the mutant neither  
245 excreted 5dR nor 7dSh (Figure 6 C, D). Instead, while undetectable in the supernatant of the  
246 wild type strain, 5dAdo strongly accumulated in the supernatant of *S. elongatus mtnP::spec<sub>R</sub>*  
247 cultures (Figure 6 B). This clearly showed that 5dR/7dSh are derived from 5dAdo in an MtnP  
248 dependent manner. Due to the detoxification via excretion, the *mtnP::spec<sub>R</sub>* mutant escapes  
249 the toxic effect of 5dAdo and does not show any growth disadvantage (Figure 6 A). It has  
250 previously been reported that a *mtnP* knockout mutant in *S. cerevisiae* as well as MtnP-  
251 deficient mammalian tumour cells excreted MTA (*Chattopadhyay et al., 2006; Kamatani and*

252 **Carson, 1980**). Both MTA and 5dAdo are known to be cleaved by MtnP (**Savarese et al., 1981**).  
253 Consistently, the *mtnP::spec<sub>R</sub>* mutant excretes MTA as well as 5dAdo (Figure 6 E). As 5dR/7dSh  
254 formation is strongly dependent on the cultivation at elevated CO<sub>2</sub> concentration we  
255 measured the amount of 5dAdo and MTA in cultures of the *mtnP::spec<sub>R</sub>* mutant supplied with  
256 ambient air or with air enriched with 2 % CO<sub>2</sub>. It turned out that the amounts of excreted  
257 5dAdo and MTA (normalized to the optical density of the cultures) are almost identical under  
258 atmospheric or elevated CO<sub>2</sub> conditions (Figure 6 E). This clearly indicates that 5dAdo salvage  
259 via 5dR/7dSh formation and excretion at high CO<sub>2</sub> conditions is not triggered by an increased  
260 synthesis of the precursor molecule 5dAdo compared to ambient CO<sub>2</sub> concentrations. Rather,  
261 it appears that 5dAdo is actively metabolised into 5dR/7dSh under elevated CO<sub>2</sub> conditions,  
262 whereas 5dAdo salvage under ambient CO<sub>2</sub> conditions is conducted by (an)other pathway(s).  
263 Since the MTA formation is also unaltered (Figure 6 E), we exclude that 5dAdo salvage via  
264 5dR/7dSh formation is triggered by an enhanced demand of MTA salvage via a bifunctional  
265 MTA/5dAdo salvage pathway.



266

267 **Figure 6: 5dAdo is cleaved by MtnP and then metabolised into 5dR and 7dSh in *S. elongatus***  
268 **at high CO<sub>2</sub> concentrations.** Growth (A), concentrations of 5dAdo (B), 5dR (C) and 7dSh (D) in  
269 the supernatant of *S. elongatus* wild type (black dots) or *mtnP::spec<sub>R</sub>* mutant (grey squares).  
270 All cultures were aerated with air supplemented with 2 %CO<sub>2</sub>. Note the different values of the  
271 y-axis. (E) 5dAdo and MTA concentrations in the supernatant of the *mtnP::spec<sub>R</sub>* mutant  
272 normalised on the optical density after 11 days of cultivation (cultures were either aerated  
273 with atmospheric air (black) or with air supplemented with 2 % CO<sub>2</sub> (grey)). Values shown in  
274 the graphs represent mean and standard deviation of three biological replicates.

275 **5dR and 7dSh formation is not ubiquitous**

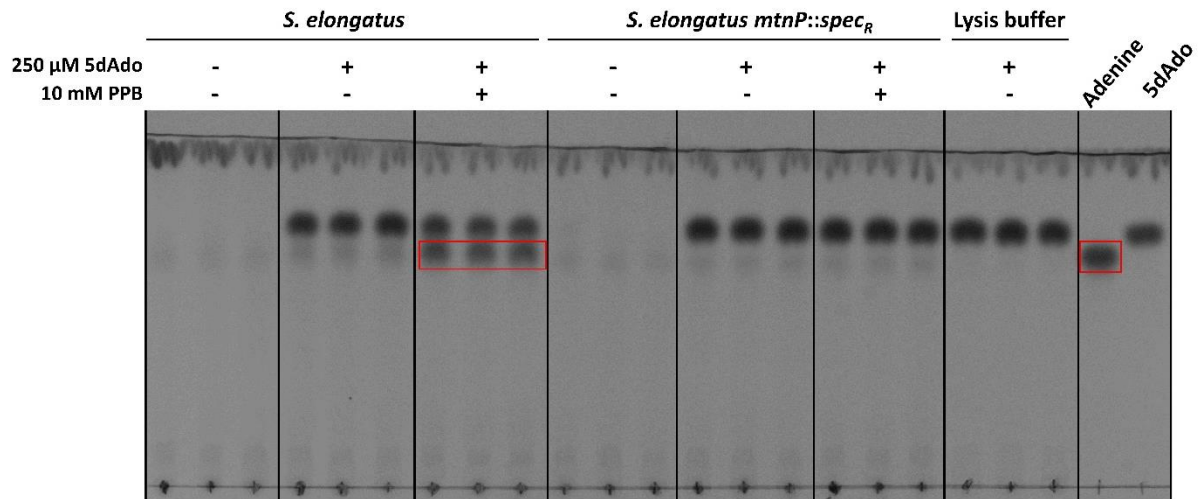
276 To clarify how widespread the synthesis of 7dSh or 5dR is in cyanobacteria, we analysed the  
277 supernatants of other cyanobacterial strains via GC-MS (*Synechococcus* sp. PCC 6301,  
278 *Synechococcus* sp. PCC 7002, *Synechococcus* sp. PCC 6312, *Synechococcus* sp. PCC 7502,  
279 *Synechocystis* sp. PCC 6803, *Anabaena variabilis* ATCC 29413, *Nostoc punctiforme*  
280 ATCC 29133, *Anabaena* sp. PCC 7120). Only in three of five *Synechococcus* strains, the  
281 deoxy-sugars 5dR and 7dSh were detectable in the supernatant. All the other strains  
282 accumulated neither 5dR nor 7dSh. In the freshwater strain *Synechococcus* sp. PCC 6301, the  
283 amounts of 7dSh and 5dR were in a similar concentration range to those in *S. elongatus*. This  
284 is not surprising since the genome of *Synechococcus* sp. PCC 6301 is nearly identical to that of  
285 *S. elongatus* PCC 7942 (*Sugita et al., 2007*). Very small amounts of 5dR and 7dSh were  
286 detected in the marine strain *Synechococcus* sp. PCC 7002. In *Streptomyces setonensis*, which  
287 was shown to produce 7dSh (*Brilisauer et al., 2019; Ito et al., 1971*), we detected  $113 \pm 7 \mu\text{M}$   
288 7dSh but no 5dR in the supernatant of cultures grown for 7 days.

289

290 **5dAdo cleavage is strictly dependent on phosphorylase activity**

291 To further characterize the cleavage of 5dAdo in *S. elongatus*, a crude extract assay was  
292 performed. Crude extracts of *S. elongatus* wild type and *mtnP::spec<sub>R</sub>* mutant cells were  
293 incubated with 5dAdo in the presence or absence of potassium phosphate buffer (PPB).  
294 Analysis of the extracts via thin layer chromatography revealed that 5dAdo cleavage and,  
295 thereby, adenine release is strictly dependent on the presence of phosphate (Figure 7).  
296 Adenine is only released by *S. elongatus* cell extracts in the presence of potassium phosphate  
297 buffer (red label), but not by *mtnP::spec<sub>R</sub>* mutant cells, which are not capable of 5dAdo  
298 cleavage. Therefore, 5dAdo cleavage in *S. elongatus* is strictly dependent on the presence of  
299 the MTA phosphorylase. Other enzymes, for example purine nucleosidase phosphorylases  
300 (*Lee et al., 2004*), apparently do not process 5dAdo in the *S. elongatus* cell extract. This result  
301 implies that the first product of 5dAdo cleavage must be 5dR-1P, which is subsequently  
302 converted into 5dR. 5dR-1P seemed quite stable because liquid chromatography (LC)-MS  
303 analysis revealed that a compound with a *m/z* ratio that corresponds to the sum formula of  
304 5dR-1P ([M+H, M+Na]<sup>+</sup> (*m/z* 215.0315; 237.0135)) accumulated in the crude extract  
305 (Figure S2). Furthermore, no 5dR formation was observed in the crude extracts (Figure S3).

306 With this, we exclude a spontaneous hydrolysis of 5dR-1P which is in accordance to the  
307 literature, where 5dR-1P is reported to be metabolically stable (*Plagemann and Wohlhueter,*  
308 *1983*).



309  
310 **Figure 7: 5dAdo cleavage in *S. elongatus* is phosphate dependent.** Crude extracts from  
311 *S. elongatus* or *S. elongatus mtnP::spec<sub>R</sub>* were incubated with 5dAdo in the presence or  
312 absence of potassium phosphate buffer (PPB) and then analysed via thin layer  
313 chromatography on silica gel. 5dAdo ( $R_f=0.68$ ) and adenine ( $R_f=0.76$ ) analytes were visualized  
314 via absorption at 254 nm. Pure adenine and 5dAdo were used as standards (right). Spots  
315 corresponding to adenine are highlighted with a red box. Three independent replicates are  
316 shown for each condition. The stability of 5dAdo in the buffer is shown with the lysis buffer  
317 control.

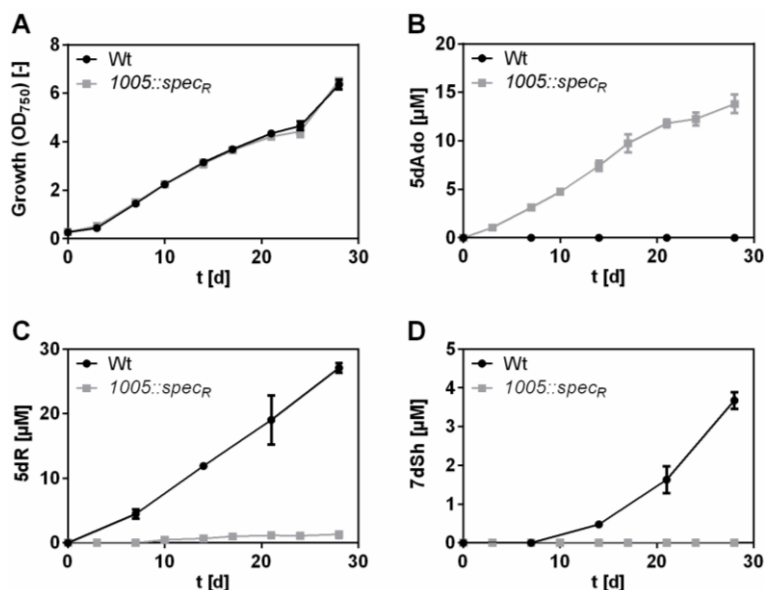
318

### 319 **5dR-1P is dephosphorylated by a specific phosphatase**

320 As 5dR-1P is metabolically stable we assumed the involvement of a specific phosphatase in  
321 5dR-1P dephosphorylation. The dephosphorylation of 5dR-1P in 5dAdo salvage is surprising as  
322 in the literature it is suggested that the phosphorylation of 5dR is essential for its further  
323 metabolization (*Beaudoin et al., 2018; North et al., 2020; Sekowska et al., 2018*). To identify  
324 the responsible phosphatase, we analysed the genome of *S. elongatus* regarding the presence  
325 of phosphoric monoester hydrolases (see Table S3, Supporting information).  
326 *Synpcc7942\_1005*, which is annotated as glucose-1-phosphatase, belonging to the haloacid  
327 dehalogenase (HAD)-like hydrolase superfamily subfamily IA (*Burroughs et al., 2006; Koonin*  
328 *and Tatusov, 1994*), seemed a promising candidate as only *S. elongatus* and *Synechococcus* sp.  
329 PCC 6301, which both produce larger amounts of 5dR/7dSh, possess a homologous gene. The  
330 other cyanobacteria mentioned above do not possess it. Furthermore, phosphatases from the



331 HAD-like hydrolase superfamily are known to be promiscuous enzymes dephosphorylating  
332 various phosphate-sugars (*Kuznetsova et al., 2006; Pradel and Boquet, 1988*). To examine  
333 whether this gene is essential for 5dR-1P dephosphorylation or 5dR/7dSh synthesis, an  
334 insertion mutant of this gene was created by the replacement with a spectinomycin resistance  
335 cassette (*S. elongatus Synpcc7942\_1005::spec<sub>R</sub>*). Under 5dR/7dSh production conditions (air  
336 supplemented with 2 % CO<sub>2</sub>) the mutant grew like the wildtype (Figure 8 A). Whereas the  
337 wildtype excretes 5dR and 7dSh, the mutant only excretes minor amounts of 5dR and no 7dSh  
338 (Figure 8 C, D). Instead, the mutant excreted 5dAdo, which was never detected in the  
339 supernatant of the wildtype (Figure 8 B). This clearly shows that the gene product of  
340 *Synpcc7942\_1005* is the major enzyme for the dephosphorylation of 5dR-1P. However, since  
341 even in the mutant small quantities of 5dR were detectable, we suggest that in addition to the  
342 gene product of *Synpcc7942\_1005* other phosphatases may contribute to residual 5dR-1P  
343 dephosphorylation. In agreement with this conclusion, we found that *Synechococcus* sp.  
344 PCC 7002, which does not possess a homolog of *Synpcc7942\_1005* also excreted minor  
345 amounts of 5dR and 7dSh (see above).



346  
347 **Figure 8: 5dR-1P is dephosphorylated by a phosphatase from the HAD hydrolase superfamily**  
348 **(*Synpcc7942\_1005*, EC 3.1.3.10)**. Growth (A), concentrations of 5dAdo (B), 5dR (C) and 7dSh  
349 (D) in the supernatant of *S. elongatus* wild type (black dots) or *1005::spec<sub>R</sub>* mutant (grey  
350 squares). All cultures were aerated with air supplemented with 2 %CO<sub>2</sub>. Note the different  
351 values of the y-axis. Values shown in the graphs represent mean and standard deviation of  
352 three biological replicates.

353 **5dR/7dSh producers possess complete MSP gene clusters**

354 By analysing the genomes of all examined cyanobacteria in this study, it turned out that those  
355 strains that do not produce 5dR and 7dSh only possess annotated genes for the first two  
356 reactions of the MSP (*mtnP* and *mtnA*), whereas the producer strains possess annotated genes  
357 for the whole MSP pathway (Table S1). The 5dAdo salvage via the DHAP shunt requires a  
358 specific class II aldolase, e.g. *DrdA* in *B. thuringiensis* (**Beaudoin et al., 2018**) or *Ald2* in  
359 *R. rubrum* (**North et al., 2020**), which is clustered with the first enzymes of the MSP, e.g. *MtnP*  
360 or *MtnN/MtnK* and *MtnA* in *R. rubrum*) or with a specific phosphorylase and isomerase as  
361 shown for *B. thuringiensis*. *In vitro* data suggest that the MTRu-1P-dehydratase (*MtnB*) from  
362 the MSP can also act as a promiscuous aldolase thereby completing the 5dAdo salvage via the  
363 DHAP shunt (**Beaudoin et al., 2018; North et al., 2020**). Since none of the analysed strains  
364 possesses such an *Ald2* homolog, we assume that 5dR/7dSh producing strains might use the  
365 DHAP shunt by using *MtnB* under certain conditions. The 5dR/7dSh non-producer strains must  
366 employ another pathway of 5dAdo salvage or use another aldolase for the DHAP shunt.



## 367 Discussion

368 Radical SAM enzymes are important enzymes in all domains of life (*Sofia et al., 2001*). A  
369 byproduct of the activity of these enzymes is 5dAdo (*Wang and Frey, 2007*). Its accumulation  
370 inhibits the activity of the radical SAM enzymes themselves (*Challand et al., 2009; Choi-Rhee*  
371 *and Cronan, 2005; Farrar et al., 2010; Palmer and Downs, 2013*). Therefore, 5dAdo salvage  
372 pathways are essential. In this study we showed that the unicellular cyanobacterium  
373 *S. elongatus* PCC 7942 has a special salvage route for 5dAdo, which was never reported before  
374 (Figure 1 A). We show that 5dAdo salvage can be achieved by the excretion of 5-deoxyribose  
375 and 7-deoxysedoheptulose. 5dR as a product of 5dAdo cleavage was postulated (*Parveen and*  
376 *Cornell, 2011; Sekowska et al., 2018*) or observed before but only in *in vitro* assays (*Choi-Rhee*  
377 *and Cronan, 2005; Sekowska et al., 2018*). Beaudoin and coworkers suggested 5dR excretion  
378 as a detoxification strategy for organisms that do not possess a specific gene cluster for 5dAdo  
379 salvage (*Beaudoin et al., 2018*) (analogous to MTR excretion in *E. coli* which does not possess  
380 a complete MSP (*Hughes, 2006; Schroeder et al., 1972*)). Therefore, 5dR accumulation in the  
381 supernatant of *S. elongatus* as an *in vivo* phenomenon was first reported by our previous  
382 publication (*Brilisauer et al., 2019*), and here identified as a result of 5dAdo salvage.

383 We propose the following model for a possible 5dAdo salvage route in *S. elongatus* by the  
384 activity of promiscuous enzymes leading to the synthesis of the bioactive deoxy-sugars 5dR  
385 and 7dSh (Figure 1 A). In brief, 5dAdo is processed by the promiscuous MTA phosphorylase  
386 into 5dR-1P. Under elevated CO<sub>2</sub> conditions, this molecule is dephosphorylated to 5dR by a  
387 potentially promiscuous phosphatase to 5dR, part of which is excreted and part of which is  
388 further metabolized by the activity of a promiscuous transketolase to 7dSh, which is also  
389 excreted from the cells to avoid its inhibitory effects on the shikimate pathway (*Brilisauer et*  
390 *al., 2019*). 7dSh is a potent inhibitor of the dehydroquinate synthase, but the inhibitory effect  
391 of the compound is dependent on the organism. The producer strain tolerates high  
392 concentrations of 7dSh (Figure 3), whereas f.e. *A. variabilis* is highly sensitive towards 7dSh  
393 treatment (*Brilisauer et al., 2019*), suggesting that 7dSh is a potent allelopathic inhibitor.

394 Although most bacteria possess the enzymes for a two-step reaction of 5dAdo cleavage (MTA  
395 nucleoside and MTR kinase) (*Albers, 2009; Zappia et al., 1988*), all examined cyanobacteria  
396 possess a MTA phosphorylase (MtnP) (Table S1), which is normally present in eukaryotes  
397 (except for plants). The phenotype of the insertion mutant (*mtnP::spec<sub>R</sub>*), which excretes

398 5dAdo instead of 5dR/7dSh, demonstrates that 5dR and 7dSh are products of 5dAdo salvage  
399 (Figure 6). The 5dAdo salvage routes previously reported suggest that the phosphorylation of  
400 5dR or the 5dR moiety of 5dAdo is essential to further metabolise the molecules via specific  
401 enzymes or by promiscuous activity of the enzymes of the MSP (**Beaudoin et al., 2018; North**  
402 **et al., 2020; Sekowska et al., 2018**). In *S. elongatus* however, 5dR-1P is subsequently  
403 dephosphorylated to 5dR for excretion or for further processing to 7dSh. Our data imply that  
404 the dephosphorylation of 5dR-1P is not due to spontaneous hydrolysis but is mainly conducted  
405 by the gene product of *Synpcc7942\_1005* (see Figure 8). *Synpcc7942\_1005* belongs to Mg<sup>2+</sup>-  
406 dependent class IA HAD-like hydrolase superfamily (**Burroughs et al., 2006**) and is annotated  
407 as a glucose-1-phosphatase, which catalyses the dephosphorylation of glucose 1-phosphate  
408 (**Turner and Turner, 1960**). As these phosphatases can also exhibit phytase activity (**Herter et**  
409 **al., 2006; Suleimanova et al., 2015**) we assume that the gene product of *Synpcc7942\_1005*  
410 might also exhibits promiscuous activity, including 5dR-1P dephosphorylation. The  
411 dephosphorylation of a similar molecule (5-fluoro-5-deoxyribose 1-phosphate) by a specific  
412 phosphoesterase (FdrA) is also conducted by *Streptomyces* sp. MA37 during the production of  
413 a specific secondary fluorometabolite (**Ma et al., 2015**) (pathway shown in Figure S4).

414 In later growth phases, small amounts of 5dR are transformed into 7dSh which is then also  
415 immediately excreted into the supernatant (Figure 2 C, Figure 4 C, E). In our previous work we  
416 showed that the affinity of *S. elongatus* transketolase for 5dR ( $k_m=108.3$  mM) is 100-fold lower  
417 than for the natural substrate D-ribose-5-phosphate ( $k_m=0.75$  mM) (**Brilisauer et al., 2019**).  
418 This is in accordance with the fact that 7dSh is only formed when relatively high extracellular  
419 5dR concentrations are reached (either in later growth phases or due to the addition of  
420 externally added 5dR; note that 5dR is continuously imported and exported). Furthermore,  
421 only one tenth of <sup>13</sup>C<sub>5</sub>-5dR is converted into <sup>13</sup>C<sub>5</sub>-7dSh. 7dSh formation from 5dR is therefore  
422 an impressive example how a more potent “derivative” (7dSh) is formed by promiscuous  
423 enzyme activity. Interestingly, a promiscuous transketolase reaction was also suggested in  
424 later steps of anaerobic 5dAdo salvage in *M. jannaschii*, in which 5dRu-1P is cleaved into  
425 lactaldehyde and methylglyoxal (**Miller et al., 2018**). *Streptomyces setonensis* (not yet  
426 sequenced) accumulates much higher concentrations of 7dSh in the supernatant than  
427 *S. elongatus* but no 5dR at all, which supports the hypothesis that 7dSh might be derived from  
428 complete conversion of 5dR by a more specific transketolase.

429 In high concentrations, 5dR exhibited toxicity towards the producer strain (Figure 3). 5dR  
430 toxicity was also reported in *B. thuringiensis* (**Beaudoin et al., 2018**), but the intracellular  
431 target is not yet known. Therefore, *S. elongatus* has to steadily excrete 5dR into the  
432 supernatant to avoid intracellular toxicity. Because  $^{13}\text{C}_5$ -5dR is taken up at the same time as  
433 unlabelled 5dR is excreted (Figure 4 B, D), it is obvious that 5dR is continuously imported and  
434 exported so that hardly any 5dR accumulates intracellularly (see Figure S1). We also assume  
435 that 7dSh is im- and exported, too. This suggests the presence of an effective export system  
436 which is essential for the survival of the producer strain.

437 5dAdo salvage via 5dR and 7dSh excretion was only observed when cultures were aerated  
438 with air supplemented with 2 %  $\text{CO}_2$  (Figure 2 B, C). Since equal amounts of 5dAdo were  
439 formed under ambient  $\text{CO}_2$  as under high  $\text{CO}_2$  conditions (Figure 6 E), we assumed that under  
440 ambient  $\text{CO}_2$  conditions 5dAdo salvage is conducted via (an)other pathway(s). The occurrence  
441 of (an) additional 5dAdo salvage pathway(s) in *S. elongatus* is underlined by the fact that  
442 5dAdo is not completely metabolised into 5dR/7dSh even under high  $\text{CO}_2$  conditions  
443 (Figure 5). Because *S. elongatus* and the other 5dR/7dSh producers are equipped with the  
444 enzymes for the whole MSP (see Table S1), we hypothesize that 5dAdo can be also  
445 metabolised via promiscuous activity of the enzymes of the MSP via the “DHAP-shunt”  
446 resulting in the formation of DHAP and acetaldehyde (see Figure 1 A, C) as suggested for  
447 organisms that do not possess a specific gene cluster for 5dAdo salvage (**Beaudoin et al., 2018**;  
448 **North et al., 2020**; **Sekowska et al., 2018**). The formation of MTA, the starting molecule of the  
449 MSP, is almost identical under atmospheric and high carbon conditions (Figure 6 E). This  
450 indicates that 5dAdo salvage via 5dR/7dSh excretion under high  $\text{CO}_2$  conditions is not  
451 triggered by an increased demand of MTA salvage. It is known that intracellular  $\text{CO}_2/\text{HCO}_3^-$  ( $\text{C}_i$ )  
452 exhibits regulatory functions at the metabolic and transcriptomic level (**Blombach and Takors,**  
453 **2015**):  $\text{CO}_2/\text{HCO}_3^-$  can alter physiochemical enzyme properties and it is known to regulate  
454 virulence and toxin production in pathogens, e.g. in *Vibrio cholerae* (**Abuaita and Withey,**  
455 **2009**). In particular, cyanobacteria strongly respond to the ambient  $\text{C}_i$  supply by a multitude  
456 of metabolic adaptations such as carbon concentrating mechanisms (**Burnap et al., 2015**) and  
457 the synthesis of cAMP (**Selim et al., 2018**). As we hypothesize that the fate of 5dAdo is a  
458 regulated process, we assume that the dephosphorylation of 5dR and the subsequent  
459 formation of 7dSh molecules is not an “accident”. They are rather purposely formed

460 metabolites, which however derive from toxic byproducts of the primary metabolism. The  
461 regulation how 5dAdo is directed towards 5dR/7dSh formation has to be further investigated.

462 With 18 radical SAM enzymes (see Table S2), *S. elongatus* only possesses a relatively small  
463 number of radical SAM enzymes compared to other prokaryotes (*B. thuringiensis*: 15; other  
464 Firmicutes: more than 40 (**Beaudoin et al., 2018**), *R. rubrum*: 25, *M. jannaschii*: 30 (**North et**  
465 **al., 2020**)). Probably the most important radical SAM enzymes under the cultivation  
466 conditions applied here are involved in cofactor biosynthesis: Lipoic acid synthase (LipA),  
467 biotin synthase (BioB) and GTP 3',8-cyclase (MoaA), which is involved in molybdopterin  
468 biosynthesis. These cofactors are presumably equally important under atmospheric or high  
469 carbon conditions resulting in the unaltered 5dAdo formation, thereby explaining the  
470 unaltered rate of 5dAdo formation.

471 7dSh can inhibit the growth of other cyanobacteria but also of plants, and was therefore  
472 suggested to be an allelopathic inhibitor by inhibiting the dehydroquinate synthase, the  
473 second enzyme of the shikimate pathway (**Brilisauer et al., 2019**). Additionally, 5dR is toxic for  
474 various organisms (Figure 3, (**Beaudoin et al., 2018**)). Despite the low concentrations of  
475 5dR/7dSh observed under laboratory conditions it is imaginable that excretion of 5dR and  
476 7dSh plays a role in protecting the ecological niche of the producer strains. 7dSh is a more  
477 potent inhibitor for example for *A. variabilis* than for the producer strain. A bactericidal effect  
478 for *A. variabilis* was observed at concentrations of 13  $\mu$ M 7dSh (**Brilisauer et al., 2019**),  
479 whereas *S. elongatus* is affected by 100  $\mu$ M (see Figure 3). In its natural environment,  
480 *S. elongatus* is able to form biofilms (**Golden, 2019; Yang et al., 2018**). In biofilms  
481 cyanobacteria tend to excrete exopolysaccharides (**Rossi and Philippis, 2015**) which can be  
482 used as a carbon source by heterotrophic members of the microbial community thereby  
483 causing locally elevated CO<sub>2</sub> concentrations. This could lead to a local enrichment of 5dR and  
484 7dSh, thereby providing a growth advantage to the producer strains protecting their niches  
485 against competing microalgae.

486

## 487 **Conclusion**

488 5dAdo salvage is a less noticeable and overlooked research topic in comparison to methionine  
489 salvage from MTA. Hence, it should be further investigated above all because 5dAdo is present  
490 in all domains of life whereas MTA is only produced by specific organisms. It is possible that

491 additional metabolites, apart from 7dSh, are derived from 5dAdo salvage in other organisms.  
492 This study shows that enzyme promiscuity is especially important for organisms with a small  
493 genome, since it enables them to produce special metabolites in absence of *ad hoc*  
494 biosynthetic gene clusters.

## 495 **Materials and Methods**

### 496 **Cultivation**

497 *Synechococcus elongatus* PCC 7942 was cultivated under photoautotrophic conditions in  
498 BG11 medium (**Rippka et al., 1979**) supplemented with 5 mM NaHCO<sub>3</sub>. Precultures were  
499 cultivated in shaking flasks at 30-50 μE at 125 rpm (27 °C). Main cultures were cultivated in  
500 500-700 mL BG11 at 27 °C in flasks which were either aerated with air or air supplemented  
501 with 2 % CO<sub>2</sub>. For this purpose, cultures were inoculated with an optical density (OD<sub>750</sub>) of 0.2-  
502 0.5 and then cultivated for the first three days at 10 μE (Lumilux de Lux, Daylight, Osram).  
503 Later, the light intensity was set to around 30 μE. Growth was determined by measuring the  
504 optical density at 750 nm (Specord 205, Analytik Jena). For feeding experiments the cultures  
505 were supplemented at the beginning of the cultivation with 5dR, [U-<sup>13</sup>C<sub>5</sub>]-5dR or  
506 5-deoxyadenosine (5dAdo; Carbosynth Ltd.) at the respective concentrations (see Results  
507 section). The other cyanobacterial strains (*Synechococcus* sp. PCC 6301, *Synechococcus* sp.  
508 PCC 6312, *Synechococcus* sp. PCC 7502, *Synechocystis* sp. PCC 6803, *Anabaena variabilis*  
509 ATCC 29413, *Nostoc punctiforme* ATCC 29133, *Anabaena* sp. PCC 7120) were cultivated as  
510 described above. *Synechococcus* sp. PCC 7002 was cultivated in a 1:1 mixture of BG11 and  
511 ASN III + vitamin B<sub>12</sub> (10 μg/mL) (**Rippka et al., 1979**).

512 *Streptomyces setonensis* SF666 was cultivated for 7 days as described in our previous work  
513 (**Brilisaer et al., 2019**).

514

### 515 **Chemical synthesis of 5-deoxyribose and 7-deoxysedoheptulose (7dSh)**

516 5dR and [U-<sup>13</sup>C<sub>5</sub>]-5dR **5** were synthesized in a four-step synthesis based on literature (**Sairam**  
517 **et al., 2003; Zhang et al., 2013**) with additional optimization. All synthetic intermediates  
518 shown in the reaction scheme (Figure S5) were verified by thin layer chromatography (TLC),  
519 mass spectrometry and NMR. Detailed data for the <sup>13</sup>C-labelled compounds are presented in  
520 the Supplementary information. The synthesis starts with the reaction of D-ribose (Sigma) or  
521 [U-<sup>13</sup>C<sub>5</sub>]-D-ribose **1** (500.1 mg, 3.22 mmol; Eurisotop) in a 4:1 mixture of acetone:methanol  
522 with SnCl<sub>2</sub>·2 H<sub>2</sub>O (1 eq) and catalytic amounts of conc. H<sub>2</sub>SO<sub>4</sub> at 45 °C for 20 h. After cooling  
523 to room temperature, the mixture was filtered, neutralised with NaHCO<sub>3</sub> solution, once again  
524 filtered and the organic solvent was evaporated. The remaining aqueous solution was

525 extracted with ethylacetate, dried over Na<sub>2</sub>SO<sub>4</sub> and evaporated in vacuo to yield the  
526 acetonide-protected ribose **2** as a colourless oil (399.7 mg, 1.91 mmol, 59 %).

527 Envisaging the following deoxygenation reaction, the protected pentose **2** (399.7 mg,  
528 1.91 mmol) was diluted in DCM with addition of TEA (2.5 eq). After cooling on ice,  
529 mesylchloride (2.5 eq) was slowly added and then stirred for 5 h on ice. The reaction mixture  
530 was washed with 1 N HCl, ultrapure water, NaHCO<sub>3</sub> solution, NaCl solution and again with  
531 ultrapure water. The organic solvent was dried over Na<sub>2</sub>SO<sub>4</sub> and evaporated in vacuo to give  
532 **3** as a yellowish oil (556.5 mg, 1.97 mmol, 103 %, mesylchloride as impurity), which becomes  
533 crystalline at 4 °C.

534 For the reduction as the third step **3** (556.1 mg, 1.91 mmol, maximum educt amount) was  
535 diluted in DMSO. After cooling on ice NaBH<sub>4</sub> (5 eq) was added slowly. Afterwards the reaction  
536 mixture was heated slowly to 85 °C and reacting for 12 h. After cooling on ice, 5 % AcOH was  
537 added to quench remaining NaBH<sub>4</sub>. The aqueous solution was extracted with DCM, washed  
538 with ultrapure water, dried over Na<sub>2</sub>SO<sub>4</sub> and evaporated in vacuo (40 °C, 750 mbar) to get **4**  
539 as a colourless oil (357.7 mg, 1.85 mmol, 86 %).

540 Deprotecting to the target **5** was achieved by diluting the acetonide-protected ω-deoxy-sugar  
541 **4** (357.7 mg, 1.85 mmol) in 0.04 N H<sub>2</sub>SO<sub>4</sub> and heating to 85 °C for 3 h. After cooling to room  
542 temperature, the reaction mixture was neutralised with NaHCO<sub>3</sub> solution and evaporated by  
543 lyophilisation. The final product was first purified by MPLC (Gradient: start CHCl<sub>3</sub>:MeOH 10:0;  
544 end CHCl<sub>3</sub>:MeOH 7:3) and HPLC (Column: HiPlexCa, 85 °C, 250x10.7 mm, 1.5 mL/min, solvent:  
545 ultrapure water) to get [U-<sup>13</sup>C<sub>5</sub>]-5-deoxy-D-ribofuranose (**5**) as a colourless oil (115.7 mg,  
546 1.12 mmol, 61 %).

547 7dSh or [3,4,5,6,7-<sup>13</sup>C<sub>5</sub>]-7dSh were synthesized in a transketolase based reaction with 5dR or  
548 [U-<sup>13</sup>C<sub>5</sub>]-5dR as substrate as described in our previous publication (*Brilisauer et al., 2019*) with  
549 slight modifications: The reaction was performed in water instead of HEPES buffer, to ensure  
550 an enhanced stability of hydroxypyruvate (very instable in HEPES (*Kobori et al., 1992*)). The  
551 reaction was performed for 7 days and fresh hydroxypyruvate was added every day.  
552 Purification was done as described for 5dR.



## 553 **Construction of insertion mutants**

554 To create an insertion mutant of the 5'-methylthioadenosine phosphorylase (EC: 2.4.2.28,  
555 MtnP, *Synpcc7942\_0932*) and of the glucose 1-phosphate phosphatase (EC: 3.1.3.10,  
556 *Synpcc7942\_1005*) in *S. elongatus* PCC 7942 a spectinomycin resistance cassette was  
557 introduced inside the respective gene. An integrative plasmid was constructed in *E. coli* and  
558 then transformed into *S. elongatus*. For this purpose, flanking regions on both sides of the  
559 respective gene were amplified from *S. elongatus* colonies with primers adding an overlapping  
560 fragment (46\_0923\_up\_fw, 47\_0923\_up\_rev and 48\_Δ0923\_down\_fw, 49\_0923\_down\_rev  
561 for *Synpcc7942\_0923::spec<sub>R</sub>*; 85\_1005\_up\_fw, 86\_1005\_up\_rev and 87\_1005\_down\_fw,  
562 88\_1005\_down\_rev for *Synpcc7942\_1005::spec<sub>R</sub>*). The primer sequences are shown in  
563 Table S3. The spectinomycin resistance cassette was amplified with the primers 32\_Spec\_fw  
564 and 33\_Spec\_rev from a plasmid containing the resistance cassette. All PCR amplification  
565 products were introduced into a pUC19 vector cut with XbaI and PstI by using Gibson assembly  
566 (**Gibson, 2011**). The plasmid was verified by Sanger sequencing (Eurofins Genomics). The  
567 plasmid was then transformed into *S. elongatus* using natural competence. In short,  
568 *S. elongatus* cells were harvested by centrifugation, washed with 400 μL BG11 and then  
569 incubated with 1 μg DNA in the dark for 6 h (28 °C). The cells were then plated on BG11 agar  
570 plates containing 10 μg/mL spectinomycin for three days. After that, the cells were transferred  
571 to agar plates containing 20 μg/mL spectinomycin. Segregation was confirmed by colony PCR  
572 (50\_0923\_rev\_seg, 51\_0923\_fw\_seg for *Synpcc7942\_0923::spec<sub>R</sub>*; 85\_1005\_up\_fw,  
573 88\_1005\_down\_rev for *Synpcc7942\_1005::spec<sub>R</sub>*). Precultures of these strains, in the  
574 following named as *S. elongatus mtnP::spec<sub>R</sub>* or *S. elongatus 1005::spec<sub>R</sub>* were cultivated in  
575 the presence of 20 μg/mL spectinomycin. Main cultures were cultivated without antibiotic.

576

## 577 **Quantification of metabolites in the culture supernatant via GC-MS**

578 Culture supernatant was collected by centrifugation of 1.5 mL culture (16.000 x g, 10 min,  
579 4 °C). 200 μL of the supernatant were transferred into a 2 mL reaction tube and immediately  
580 frozen on liquid nitrogen and stored at -80 °C. The supernatant was lyophilized. For  
581 intracellular measurements, the cell pellets were also frozen in liquid nitrogen. The samples  
582 were extracted with 700 μL precooled CHCl<sub>3</sub>/MeOH/H<sub>2</sub>O (1/2.5/0.5 v/v/v) as described in the  
583 literature (**Fürtauer et al., 2016**) with slight modifications. Samples were homogenized by



584 vortexing, ultrasonic bath (Bandelin, Sonorex) treatment (10 min) and shaking (10 min,  
585 1.000 rpm). After that, the samples were cooled on ice for 5 min and then centrifuged (10 min,  
586 16.000 x *g*, 4 °C). The supernatant was transferred into a new reaction tube. The pellet was  
587 again extracted with 300 µL extraction solvent as described before. The supernatants were  
588 pooled and 300 µL ice cold water was added for phase separation. The samples were vortexed,  
589 incubated on ice (5 min) and then centrifuged (10 min, 16.000 x *g*, 4 °C). 900 µL of the upper,  
590 polar phase were transferred into a new 2 mL reaction tube and dried in a vacuum  
591 concentrator (Eppendorf, Concentrator plus, mode: V-AQ, 30 °C) for approximately 4.5 h. The  
592 samples were immediately closed and then derivatized as described in the literature  
593 (**Weckwerth et al., 2004**) with slight modifications. Therefore, the pellets were resolved in  
594 60 µL methoxylamine hydrochloride (Acros Organics) in pyridine (anhydrous, Sigma-Aldrich)  
595 (20 mg/mL), homogenized by vortexing, a treatment in an ultrasonic bath (15 min, RT) and an  
596 incubation at 30 °C on a shaker (1.400 rpm) for 1.5 h. After that, 80 µL *N*-methyl-*N*-  
597 (trimethylsilyl)trifluoroacetamide (MSTFA, Macherey-Nagel) was added and the samples were  
598 incubated at 37 °C for 30 min (1.200 rpm). The samples were centrifuged (16.000 x *g*, 2 min)  
599 and 120 µL were transferred into a glass vial with micro insert. The samples were stored at  
600 room temperature for 2 h before GC-MS measurement.

601 GC-MS measurements were performed on a Shimadzu GC-MS TQ 8040 (Injector: AOC-20i,  
602 Sampler: AOC-20s) with a SH-Rxi-5Sil-MS column (Restek, 30 m, 0.25 mm ID, 0.25 µm). For GC  
603 measurement, the initial oven temperature was set to 60 °C for 3 min. After that the  
604 temperature was increased by 10 °C/min up to 320 °C, which was then held for 10 min. The  
605 GC-MS interface temperature was set to 280 °C, the ion source was heated to 200 °C. The  
606 carrier gas flow (helium) was 1.28 mL/min. The injection was performed in split mode 1:10.  
607 The mass spectrometer was operated in EI mode. Metabolites were detected in MRM mode.  
608 Quantification of the metabolites was performed with a calibration curve of the respective  
609 substances (5dAdo, 5dR, 7dSh, <sup>13</sup>C<sub>5</sub>-5dR, <sup>13</sup>C<sub>5</sub>-7dSh).

610

### 611 **Quantification of MTA and 5dAdo**

612 For the quantification of MTA and 5dAdo (Figure 6 E) 25 µL of culture supernatant were mixed  
613 with 75 µL aqueous solution of 20 % MeOH (v/v) + 0.1 % (v/v) formic acid. Samples were  
614 analysed on a LC-HR-MS system (Dionex Ultimate 3000 HPLC system coupled to maXis 4G

615 ESI-QTOF mass spectrometer). 5dAdo and MTA were separated on a C18 column with a  
616 MeOH/H<sub>2</sub>O gradient (10 %-100 % in 20 min). The concentration was calculated from peak  
617 areas of extracted ion chromatograms of a calibration curve of the respective standards (MTA  
618 was obtained from Cayman Chemicals).

619

## 620 **Crude Extract Assays**

621 Crude extract assays were performed by harvesting *S. elongatus* or *S. elongatus mtnP::spec<sub>R</sub>*  
622 cultures which were cultivated at 2 % CO<sub>2</sub> supplementation until an optical density of around  
623 OD<sub>750</sub>=4 (t=14 d). 10 mL of the cultures were centrifuged (3.200 x *g*, 10 min, 4 °C), the  
624 supernatant was discarded, the pellet was washed with 10 mL fresh BG11 medium, and again  
625 centrifuged. After that, the pellet was resuspended in 2.5 mL lysis buffer (25 mM HEPES  
626 pH 7.5, 50 mM KCl, 1 mM DTT) and filled into 2 mL tubes with a screw cap. 100 µL glass beads  
627 (∅=0.1-0.11 mm) was added and the cells were then disrupted at 4 °C by a FastPrep®-24  
628 instrument (MP Biomedicals, 5 m/s, 20 sec, 3x with 5 min break). To remove the cell debris a  
629 centrifugation step was performed (25.000 x *g*, 10 min, 4 °C). 200 µL of the supernatant was  
630 used for the crude extract assay. The extract was either used alone or supplemented with  
631 10 µL 5 mM 5dAdo (final concentration: 250 µM) or in combination with 40 µl 50 mM  
632 potassium phosphate buffer (PBB) pH 7.5 (final concentration: 10 mM). The extracts were  
633 incubated at 28 °C for 7 h, then frozen in liquid nitrogen and lyophilized. 100 µL MeOH was  
634 added, the samples were homogenized and then centrifuged. 50 µL was applied on a TLC plate  
635 (ALUGRAM® Xtra SIL G UV<sub>254</sub>, Macherey-Nagel). For the mobile phase CHCl<sub>3</sub>/MeOH in a ratio  
636 of 9:5 (v/v) with 1 % (v) formic acid was used. Visualization was performed at 254 nm  
637 (Figure 7) or spraying with anisaldehyde (Figure S3).

638

## 639 **Bioinformatics**

640 Annotations of the different genes were obtained by the KEGG database (*Kanehisa and Goto,*  
641 **2000**). Also, radical SAM enzyme search was done in KEGG database (searching for pf:  
642 Radical\_SAM, PF04055). Searching for homologous genes was performed by using BlastP  
643 (BLOSUM 62). Searching for Ald2 homologs in KEGG database, *R. rubrum* protein sequence

644 (rru:Rru\_A0359) was used as a query sequence and an e-value <10e-20 was used for positive  
645 results.

646

#### 647 **Author Contributions**

648 J. R. designed, performed, interpreted experiments, and wrote the manuscript. P. R.  
649 synthesized labelled and unlabelled 5dR and 7dSh. J. K. optimized the GC-MS method and  
650 supported with GC-MS measurements. K. B supported initial experiments and proof-read  
651 manuscript. S. G. supported chemical analytics and proof-read manuscript. K. F. supervised  
652 the study and supported manuscript writing.

653

#### 654 **Acknowledgements**

655 Work of the authors is supported and funded by the “Glycobiotechnology” initiative (Ministry  
656 for Science, Research and Arts Baden-Württemberg), the RTG 1708 “Molecular principles of  
657 bacterial survival strategies” and the Institutional Strategy of the University of Tübingen  
658 (Deutsche Forschungsgemeinschaft, ZUK 63). The work was further supported by  
659 infrastructural funding from the DFG Cluster of Excellence EXC 2124 Controlling Microbes to  
660 Fight Infections. We thank Dr. Libera Lo Presti for critical reading the manuscript. We  
661 especially thank Tim Orthwein for fruitful discussions and Michaela Schuppe for the cultivation  
662 of *Streptomyces setonensis*.

663

#### 664 **Competing interests**

665 The authors declare no competing interests.

## 666 References

- 667 **Abuaita BH**, Withey JH. 2009. Bicarbonate Induces *Vibrio cholerae* virulence gene expression  
668 by enhancing ToxT activity. *Infection and Immunity* **77**:4111–4120. doi: 10.1128/IAI.00409-  
669 09.
- 670 **Albers E**. 2009. Metabolic characteristics and importance of the universal methionine  
671 salvage pathway recycling methionine from 5'-methylthioadenosine. *IUBMB Life* **61**:1132–  
672 1142. doi: 10.1002/iub.278.
- 673 **Beaudoin GAW**, Li Q, Folz J, Fiehn O, Goodsell JL, Angerhofer A, Bruner SD, Hanson AD. 2018.  
674 Salvage of the 5-deoxyribose byproduct of radical SAM enzymes. *Nature Communications*  
675 **9**:3105. doi: 10.1038/s41467-018-05589-4.
- 676 **Blombach B**, Takors R. 2015. CO<sub>2</sub> - Intrinsic Product, Essential Substrate, and Regulatory  
677 Trigger of Microbial and Mammalian Production Processes. *Frontiers in Bioengineering*  
678 *and Biotechnology* **3**. doi: 10.3389/fbioe.2015.00108.
- 679 **Booker SJ**, Grove TL. 2010. Mechanistic and functional versatility of radical SAM enzymes.  
680 *F1000 Biology Reports* **2**:52. doi: 10.3410/B2-52.
- 681 **Brilisauer K**, Rapp J, Rath P, Schöllhorn A, Bleul L, Weiß E, Stahl M, Grond S, Forchhammer K.  
682 2019. Cyanobacterial antimetabolite 7-deoxy-sedoheptulose blocks the shikimate  
683 pathway to inhibit the growth of prototrophic organisms. *Nature Communications* **10**:545.  
684 doi: 10.1038/s41467-019-08476-8.
- 685 **Broderick JB**, Duffus BR, Duschene KS, Shepard EM. 2014. Radical S-adenosylmethionine  
686 enzymes. *Chemical Reviews* **114**:4229–4317. doi: 10.1021/cr4004709.
- 687 **Burnap RL**, Hagemann M, Kaplan A. 2015. Regulation of CO<sub>2</sub> Concentrating Mechanism in  
688 Cyanobacteria. *Life* **5**:348–371. doi: 10.3390/life5010348.
- 689 **Burroughs AM**, Allen KN, Dunaway-Mariano D, Aravind L. 2006. Evolutionary genomics of  
690 the HAD superfamily: understanding the structural adaptations and catalytic diversity in a  
691 superfamily of phosphoesterases and allied enzymes. *Journal of Molecular Biology*  
692 **361**:1003–1034. doi: 10.1016/j.jmb.2006.06.049.
- 693 **Challand MR**, Ziegert T, Douglas P, Wood RJ, Kriek M, Shaw NM, Roach PL. 2009. Product  
694 inhibition in the radical S-adenosylmethionine family. *FEBS Letters* **583**:1358–1362.  
695 doi: 10.1016/j.febslet.2009.03.044.
- 696 **Chattopadhyay MK**, Tabor CW, Tabor H. 2006. Methylthioadenosine and polyamine  
697 biosynthesis in a *Saccharomyces cerevisiae* *meu1Δ* mutant. *Biochemical and Biophysical*  
698 *Research Communications* **343**:203–207. doi: 10.1016/j.bbrc.2006.02.144.
- 699 **Choi-Rhee E**, Cronan JE. 2005. A Nucleosidase Required for In Vivo Function of the S-  
700 Adenosyl-L-Methionine Radical Enzyme, Biotin Synthase. *Chemistry & Biology* **12**:589–593.  
701 doi: 10.1016/j.chembiol.2005.04.012.
- 702 **Copeland A**, Lucas S, Lapidus A, Barry K, Detter JC, Glavina T, Hammon N, Israni S, Pitluck S,  
703 Schmutz J, Larimer F, Land, M M, Kyrpides N, Lykidis A, Golden S, Richardson P. 2014.  
704 Complete sequence of chromosome 1 of *Synechococcus elongatus* PCC 7942.
- 705 **Farrar CE**, Siu KKW, Howell PL, Jarrett JT. 2010. Biotin synthase exhibits burst kinetics and  
706 multiple turnovers in the absence of inhibition by products and product-related  
707 biomolecules. *Biochemistry* **49**:9985–9996. doi: 10.1021/bi101023c.
- 708 **Fontecave M**, Atta M, Mulliez E. 2004. S-adenosylmethionine: nothing goes to waste. *Trends*  
709 *in Biochemical Sciences* **29**:243–249. doi: 10.1016/j.tibs.2004.03.007.
- 710 **Fürtauer L**, Weckwerth W, Nägele T. 2016. A Benchtop Fractionation Procedure for  
711 Subcellular Analysis of the Plant Metabolome. *Frontiers in Plant Science* **7**.  
712 doi: 10.3389/fpls.2016.01912.

- 713 **Gibson DG**. 2011. Enzymatic Assembly of Overlapping DNA Fragments. In: Voigt C, ed.  
714 *Methods in Enzymology: Synthetic Biology, Part B*. Academic Press.
- 715 **Golden SS**. 2019. The international journeys and aliases of *Synechococcus elongatus*. *New*  
716 *Zealand Journal of Botany* **57**:70–75. doi: 10.1080/0028825X.2018.1551805.
- 717 **Herter T**, Berezina OV, Zinin NV, Velikodvorskaya GA, Greiner R, Borriss R. 2006. Glucose-1-  
718 phosphatase (AgpE) from *Enterobacter cloacae* displays enhanced phytase activity.  
719 *Applied Microbiology and Biotechnology* **70**:60–64. doi: 10.1007/s00253-005-0024-8.
- 720 **Holliday GL**, Akiva E, Meng EC, Brown SD, Calhoun S, Pieper U, Sali A, Booker SJ, Babbitt PC.  
721 2018. Atlas of the Radical SAM Superfamily: Divergent Evolution of Function Using a “Plug  
722 and Play” Domain. *Methods in Enzymology* **606**:1–71. doi: 10.1016/bs.mie.2018.06.004.
- 723 **Hughes JA**. 2006. In vivo hydrolysis of S-adenosyl-L-methionine in *Escherichia coli* increases  
724 export of 5-methylthioribose. *Canadian Journal of Microbiology* **52**:599–602.  
725 doi: 10.1139/w06-008.
- 726 **Ito T**, Ezaki N, Tsuruoka T, Niida T. 1971. Structure of SF-666 A and SF-666 B, new  
727 monosaccharides. *Carbohydrate Research* **17**:375–382. doi: 10.1016/S0008-  
728 6215(00)82545-8.
- 729 **Kamatani N**, Carson DA. 1980. Abnormal regulation of methylthioadenosine and polyamine  
730 metabolism in methylthioadenosine phosphorylase-deficient human leukemic cell lines.  
731 *Cancer Research* **40**:4178–4182.
- 732 **Kanehisa M**, Goto S. 2000. KEGG: Kyoto Encyclopedia of Genes and Genomes. *Nucleic Acids*  
733 *Research* **28**:27–30. doi: 10.1093/nar/28.1.27.
- 734 **Kobori Y**, Myles DC, Whitesides GM. 1992. Substrate specificity and carbohydrate synthesis  
735 using transketolase. *The Journal of Organic Chemistry* **57**:5899–5907.  
736 doi: 10.1021/jo00048a023.
- 737 **Koonin EV**, Tatusov RL. 1994. Computer analysis of bacterial haloacid dehalogenases defines  
738 a large superfamily of hydrolases with diverse specificity. Application of an iterative  
739 approach to database search. *Journal of Molecular Biology* **244**:125–132.  
740 doi: 10.1006/jmbi.1994.1711.
- 741 **Kuznetsova E**, Proudfoot M, Gonzalez CF, Brown G, Omelchenko MV, Borozan I, Carmel L,  
742 Wolf YI, Mori H, Savchenko AV, Arrowsmith CH, Koonin EV, Edwards AM, Yakunin AF.  
743 2006. Genome-wide analysis of substrate specificities of the *Escherichia coli* haloacid  
744 dehalogenase-like phosphatase family. *The Journal of Biological Chemistry* **281**:36149–  
745 36161. doi: 10.1074/jbc.M605449200.
- 746 **Lee JE**, Settembre EC, Cornell KA, Riscoe MK, Sufrin JR, Ealick SE, Howell PL. 2004. Structural  
747 comparison of MTA phosphorylase and MTA/AdoHcy nucleosidase explains substrate  
748 preferences and identifies regions exploitable for inhibitor design. *Biochemistry* **43**:5159–  
749 5169. doi: 10.1021/bi035492h.
- 750 **Li B**, Sher D, Kelly L, Shi Y, Huang K, Knerr PJ, Joewono I, Rusch D, Chisholm SW, van der Donk  
751 WA. 2010. Catalytic promiscuity in the biosynthesis of cyclic peptide secondary  
752 metabolites in planktonic marine cyanobacteria. *Proceedings of the National Academy of*  
753 *Sciences* **107**:10430–10435. doi: 10.1073/pnas.0913677107.
- 754 **Ma L**, Bartholome A, Tong MH, Qin Z, Yu Y, Shepherd T, Kyeremeh K, Deng H, O'Hagan D.  
755 2015. Identification of a fluorometabolite from *Streptomyces* sp. MA37: (2R3S4S)-5-fluoro-  
756 2,3,4-trihydroxypentanoic acid. *Chemical Science* **6**:1414–1419. doi: 10.1039/C4SC03540B.
- 757 **Marsh ENG**, Patterson DP, Li L. 2010. Adenosyl Radical: Reagent and Catalyst in Enzyme  
758 Reactions. *ChemBioChem* **11**:604–621. doi: 10.1002/cbic.200900777.



- 759 **Miller DV**, Rauch BJ, Harich K, Xu H, Perona JJ, White RH. 2018. Promiscuity of methionine  
760 salvage pathway enzymes in *Methanocaldococcus jannaschii*. *Microbiology* **164**:969–981.  
761 doi: 10.1099/mic.0.000670.
- 762 **North JA**, Wildenthal JA, Erb TJ, Evans BS, Byerly KM, Gerlt JA, Tabita FR. 2020. A bifunctional  
763 salvage pathway for two distinct *S*-adenosylmethionine by-products that is widespread in  
764 bacteria, including pathogenic *Escherichia coli*. *Molecular Microbiology* **113**:923–937.  
765 doi: 10.1111/mmi.14459.
- 766 **Palmer LD**, Downs DM. 2013. The thiamine biosynthetic enzyme ThiC catalyzes multiple  
767 turnovers and is inhibited by *S*-adenosylmethionine (AdoMet) metabolites. *Journal of*  
768 *Biological Chemistry* **288**:30693–30699. doi: 10.1074/jbc.M113.500280.
- 769 **Parveen N**, Cornell KA. 2011. Methylthioadenosine/*S*-adenosylhomocysteine nucleosidase, a  
770 critical enzyme for bacterial metabolism. *Molecular Microbiology* **79**:7–20.  
771 doi: 10.1111/j.1365-2958.2010.07455.x.
- 772 **Plagemann PG**, Wohlueter RM. 1983. 5'-Deoxyadenosine metabolism in various  
773 mammalian cell lines. *Biochemical Pharmacology* **32**:1433–1440. doi: 10.1016/0006-  
774 2952(83)90458-6.
- 775 **Pradel E**, Boquet PL. 1988. Acid phosphatases of *Escherichia coli*: molecular cloning and  
776 analysis of *agg*, the structural gene for a periplasmic acid glucose phosphatase. *Journal of*  
777 *Bacteriology* **170**:4916–4923. doi: 10.1128/jb.170.10.4916-4923.1988.
- 778 **Rippka R**, Deruelles J, Waterbury JB, Herdman M, Stanier RY. 1979. Generic Assignments,  
779 Strain Histories and Properties of Pure Cultures of Cyanobacteria. *Journal of General*  
780 *Microbiology* **111**:1–61. doi: 10.1099/00221287-111-1-1.
- 781 **Rossi F**, Philippis R de. 2015. Role of cyanobacterial exopolysaccharides in phototrophic  
782 biofilms and in complex microbial mats. *Life* **5**:1218–1238. doi: 10.3390/life5021218.
- 783 **Sairam P**, Puranik R, Sreenivasa Rao B, Veerabhadra Swamy P, Chandra S. 2003. Synthesis of  
784 1,2,3-tri-*O*-acetyl-5-deoxy-*D*-ribofuranose from *D*-ribose. *Carbohydrate Research* **338**:303–  
785 306. doi: 10.1016/S0008-6215(02)00464-0.
- 786 **Savarese TM**, Crabtree GW, Parks RE. 1981. 5'-methylthioadenosine phosphorylase—I:  
787 Substrate activity of 5'-deoxyadenosine with the enzyme from Sarcoma 180 cells.  
788 *Biochemical Pharmacology* **30**:189–199. doi: 10.1016/0006-2952(81)90077-0.
- 789 **Schroeder HR**, Barnes CJ, Bohinski RC, Mumma RO, Mallette MF. 1972. Isolation and  
790 identification of 5-methylthioribose from *Escherichia coli* B. *Biochimica et Biophysica Acta*  
791 *(BBA) - General Subjects* **273**:254–264. doi: 10.1016/0304-4165(72)90215-2.
- 792 **Sekowska A**, Ashida H, Danchin A. 2018. Revisiting the methionine salvage pathway and its  
793 paralogues. *Microbial Biotechnology* **12**:77–97. doi: 10.1111/1751-7915.13324.
- 794 **Sekowska A**, Danchin A. 2002. The methionine salvage pathway in *Bacillus subtilis*. *BMC*  
795 *Microbiology* **2**:8. doi: 10.1186/1471-2180-2-8.
- 796 **Sekowska A**, Denervaud V, Ashida H, Michoud K, Haas D, Yokota A, Danchin A. 2004.  
797 Bacterial variations on the methionine salvage pathway. *BMC Microbiology* **4**:9.  
798 doi: 10.1186/1471-2180-4-9.
- 799 **Selim KA**, Haase F, Hartmann MD, Hagemann M, Forchhammer K. 2018. P<sub>II</sub>-like signaling  
800 protein SbtB links cAMP sensing with cyanobacterial inorganic carbon response.  
801 *Proceedings of the National Academy of Sciences* **115**:E4861–E4869.  
802 doi: 10.1073/pnas.1803790115.
- 803 **Shih PM**, Wu D, Latifi A, Axen SD, Fewer DP, Talla E, Calteau A, Cai F, Tandeau de Marsac N,  
804 Rippka R, Herdman M, Sivonen K, Coursin T, Laurent T, Goodwin L, Nolan M, Davenport  
805 KW, Han CS, Rubin EM, Eisen JA, Woyke T, Gugger M, Kerfeld CA. 2013. Improving the  
806 coverage of the cyanobacterial phylum using diversity-driven genome sequencing.

- 807 *Proceedings of the National Academy of Sciences* **110**:1053–1058.  
808 doi: 10.1073/pnas.1217107110.
- 809 **Sofia HJ**, Chen G, Hetzler BG, Reyes-Spindola JF, Miller NE. 2001. Radical SAM, a novel  
810 protein superfamily linking unresolved steps in familiar biosynthetic pathways with radical  
811 mechanisms: Functional characterization using new analysis and information visualization  
812 methods. *Nucleic Acids Research* **29**:1097–1106. doi: 10.1093/nar/29.5.1097.
- 813 **Sugita C**, Ogata K, Shikata M, Jikuya H, Takano J, Furumichi M, Kanehisa M, Omata T, Sugiura  
814 M, Sugita M. 2007. Complete nucleotide sequence of the freshwater unicellular  
815 cyanobacterium *Synechococcus elongatus* PCC 6301 chromosome: gene content and  
816 organization. *Photosynthesis Research* **93**:55–67. doi: 10.1007/s11120-006-9122-4.
- 817 **Suleimanova AD**, Beinbauer A, Valeeva LR, Chastukhina IB, Balaban NP, Shakirov EV, Greiner  
818 R, Sharipova MR. 2015. Novel Glucose-1-Phosphatase with High Phytase Activity and  
819 Unusual Metal Ion Activation from Soil Bacterium *Pantoea* sp. Strain 3.5.1. *Applied and  
820 Environmental Microbiology* **81**:6790–6799. doi: 10.1128/AEM.01384-15.
- 821 **Turner DH**, Turner JF. 1960. The hydrolysis of glucose monophosphates by a phosphatase  
822 preparation from pea seeds. *Biochemical Journal* **74**:486–491. doi: 10.1042/bj0740486.
- 823 **Wang SC**, Frey PA. 2007. S-adenosylmethionine as an oxidant: the radical SAM superfamily.  
824 *Trends in Biochemical Sciences* **32**:101–110. doi: 10.1016/j.tibs.2007.01.002.
- 825 **Weckwerth W**, Wenzel K, Fiehn O. 2004. Process for the integrated extraction, identification  
826 and quantification of metabolites, proteins and RNA to reveal their co-regulation in  
827 biochemical networks. *Proteomics* **4**:78–83. doi: 10.1002/pmic.200200500.
- 828 **Wray JW**, Abeles RH. 1995. The methionine salvage pathway in *Klebsiella pneumoniae* and  
829 rat liver. Identification and characterization of two novel dioxygenases. *The Journal of  
830 Biological Chemistry* **270**:3147–3153. doi: 10.1074/jbc.270.7.3147.
- 831 **Yang Y**, Lam V, Adomako M, Simkovsky R, Jakob A, Rockwell NC, Cohen SE, Taton A, Wang J,  
832 Lagarias JC, Wilde A, Nobles DR, Brand JJ, Golden SS. 2018. Phototaxis in a wild isolate of  
833 the cyanobacterium *Synechococcus elongatus*. *Proceedings of the National Academy of  
834 Sciences* **115**:E12378–E12387. doi: 10.1073/pnas.1812871115.
- 835 **Zappia V**, Della Ragione F, Pontoni G, Gragnaniello V, Carteni-Farina M. 1988. Human 5'-  
836 Deoxy-5'-Methylthioadenosine Phosphorylase: Kinetic Studies and Catalytic Mechanism.  
837 In: Zappia V, Pegg AE, eds. *Progress in Polyamine Research: Novel Biochemical,  
838 Pharmacological, and Clinical Aspects*. Springer US, Boston, MA.
- 839 **Zhang JT**, Chen SP, Feng JM, Liu DW, Tang LJ, Wang XJ, Huang SP. 2013. Synthetic Study of 1,  
840 2, 3-Tri-O-Acetyl-5-Deoxy-D-Ribofuranose. *Advanced Materials Research* **781-784**:1184–  
841 1186. doi: 10.4028/www.scientific.net/AMR.781-784.1184.